
Article:
Warren, N.J., Rosselgong, J., Madsen, J. et al. (1 more author) (2015) Disulfide-Functionalized Diblock Copolymer Worm Gels. Biomacromolecules , 16 (8). pp. 2514-2521. ISSN 1525-7797

https://doi.org/10.1021/acs.biomac.5b00767

Disulfide-Functionalized Diblock Copolymer Worm Gels

Nicholas J. Warren[†,*], Julien Rosselgong, Jeppe Madsen[†] and Steven P. Armes[*]

†Department of Chemistry, University of Sheffield, Brook Hill, Sheffield, S3 7HF, UK

ABSTRACT: Two methods for the functionalization of the outer surface of RAFT-synthesized poly(glycerol monomethacrylate)-poly(2-hydroxypropyl methacrylate) (PGMA-PHPMA, or G_x-H_y for brevity) diblock copolymer worms with disulfide groups are investigated. The first involves copolymerization of GMA with a small amount of a disulfide dimethacrylate (DSDMA, or D) to afford a G_{54} -$D_{0.50}$ macromolecular chain transfer agent (macro-CTA) under conditions that favor intramolecular cyclization and hence the formation of linear chains. Alternatively, a new disulfide-based bifunctional RAFT agent (DSDB) is used to prepare a G_{45}-S-S-G_{45}, or $(G_{45}$-$S)_2$, macro-CTA. A binary mixture of a non-functionalized G_{55} macro-CTA with each of these two macro-CTAs in turn was utilized to polymerize 2-hydroxypropyl methacrylate via RAFT aqueous dispersion polymerization. By targeting the appropriate PHPMA DP and systematically varying the macro-CTA molar ratio, it was possible to prepare diblock copolymer worm gels containing varying degrees of disulfide functionality. For both formulations, oscillatory rheology studies confirmed that higher disulfide contents led to enhanced gel strength, presumably as a result of inter-worm covalent bond formation via disulfide/thiol exchange. Using the DSDB-based macro-CTA led to the strongest worm gels, and this formulation also proved to be more effective in suppressing the thermo-sensitive behavior that is observed for the non-disulfide-functionalized control worm gel. However, macroscopic precipitation occurred when the proportion of DSDB-based macro-CTA was increased to 50 mol %, whereas the DSDMA-based macro-CTA could be utilized at up to 80 mol %. Finally, the worm gel strength could be reduced to that of a non-disulfide-containing worm gel by reductive cleavage of the inter-worm disulfide bonds using excess tris(2-carboxyethyl)phosphine (TCEP).

Introduction

Recently, polymerization-induced self-assembly (PISA) has provided a facile route to prepare a wide range of nano-objects at relatively high concentrations (up to 50% w/w solids) compared to the conditions normally utilized for conventional post-polymerization processing.[1-10] For example, detailed phase diagrams have been constructed for the reversible addition-fragmentation chain transfer (RAFT) aqueous dispersion polymerization of 2-hydroxypropyl methacrylate (HPMA) that allow pure phases of diblock copolymer spheres, worms or vesicles to be reproducibly targeted using either poly(glycerol monomethacrylate) (PGMA),[3] poly(2-(methacryloyloxy)ethyl phosphorylcholine) (PMPC),[5] poly(ethylene glycol)[11] or poly(amino acid methacrylate)[12] -based macro-CTAs. Such PISA formulations provide an excellent opportunity to investigate the physical properties of these nano-objects since their synthesis can be conducted efficiently via convenient one-pot protocols. Moreover, the weakly hydrophobic nature of the core-forming PHPMA block leads to interesting thermo-responsive behavior. For example, the worms form free-standing gels at room temperature but undergo reversible de-gelation on cooling as a result of a worm-to-sphere transition.[13,14] Analogous thermos-responsive worm gels have also been synthesized by Monteiro and co-workers. [15 16]

Thiol-ene click chemistry has become an extremely popular method for functionalizing polymers owing to its high efficiency and remarkable orthogonality, which ensures minimal formation of unwanted side-products.[17-24] Of particular relevance to the present study, RAFT-synthesized methacrylic (co)polymers possess dithiobenzoate or trithiocarbonate end-groups, which can be regarded as latent terminal thiol groups. In principle, end-group removal can be achieved by addition of a base such as a primary amine or via a radical reaction.[25,26]

However, such reactions are relatively inefficient for sterically-hindered methacrylic polymers. Moreover, derivatization

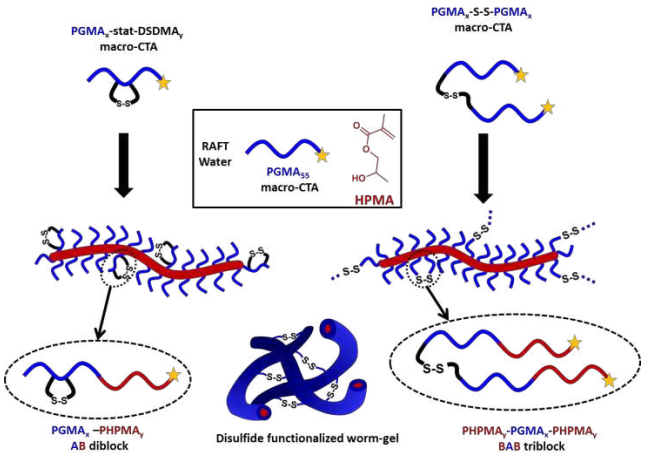

Scheme 1. Method of incorporation of disulfide functionality into PGMA-PHPMA worm gels using either a disulfide-based methacrylic comonomer or a disulfide-based RAFT chain transfer agent. Converting such disulfide groups into thiol groups enables covalently cross-linked worm gels to be obtained via reformation of inter-worm disulfide bonds.

of the active Z group poses a particular problem for block copolymer nano-objects prepared by RAFT dispersion polymerization,[27] since these terminal groups are located within the non-solvated solvatophobic block. In order to decorate the outer surface of such nano-objects, the latent functional group(s) must be located in the hydrophilic stabilizer block. This approach can either utilize the terminal R group by using an appropriate pyridyl disulfide-based CTA[28] or involve co-polymerization of a latent thiol comonomer such as disulfide dimethacrylate (DSDMA)[29] or pyridyl disulfide methacrylate.[30]

Herein we examine two routes for the production of thiol-functionalized PGMA-PHPMA diblock copolymer worms

from disulfide-based worm precursors (see Scheme 1). In principle, this approach enables the worm gel strength to be enhanced by incorporating reversible covalent cross-links between adjacent worms. The general strategy involves incorporation of a disulfide group into the hydrophilic PGMA macro-CTA that is subsequently used for the RAFT aqueous dispersion polymerization of HPMA. The first route involves statistical copolymerization of a bifunctional disulfide-based methacrylic monomer (DSDMA) with GMA during the macro-CTA synthesis.[31-33] Recently, we reported that, when copolymerized with a monofunctional methacrylic monomer in sufficiently dilute solution, DSDMA undergoes intramolecular cyclization rather than intermolecular branching.[29] Subsequent disulfide cleavage produces two 2-thioethyl methacrylate residues on the polymer backbone. This has been recently exploited by Rosselgong and co-workers to prepare thiol-functionalized vesicles.[29] The second route involves a new disulfide-based RAFT CTA. In contrast to Maynard and co-workers[28], who synthesised a monofunctional RAFT CTA bearing a pyridyl disulfide group, we use a concept similar to that described by Matyjaszewski and co-workers, who reported a bifunctional ATRP initiator containing a central disulfide bond. After (co)polymer synthesis, the latter bond can be cleaved to yield two chains each possessing terminal primary thiol groups. In related work, Li et al.[34] and Madsen et al.[35,36] designed free-standing gels consisting of ABA triblock copolymer 'flower micelles' which formed a 3D network comprising flower-like micelles inter-connected via bridging triblock copolymer chains. In this case, the central disulfide bond acts as a 'keystone': selective cleavage of such bonds caused immediate degelation to produce a free-flowing fluid composed of individual thiol-decorated micelles.

In the present work, we focus on RAFT-synthesized block copolymer worms in which the thiol groups are located at the R terminus of the chains, which is expressed at the periphery of the steric stabilizer block. In particular, we use oscillatory rheology to compare worm gel strengths and hence investigate the influence of the spatial location of the thiol groups on this parameter. We also envisage that these thiol-functional worms may provide a convenient protocol for the covalent attachment of bioactive molecules such as oligopeptides. Thiol-decorated worm gels are also expected to be muco-adhesive, which suggests some potential for drug delivery applications.[37,38]

Experimental

Materials

Glycerol monomethacrylate (GMA; 99.8 %) was donated by GEO Specialty Chemicals (Hythe, UK) and used without further purification. 2-Hydroxypropyl methacrylate (HPMA) was purchased from Alfa Aesar (Heysham, UK). 2-Cyano-2-propyl dithiobenzoate (CPDB, 80 % as judged by ^{1}H NMR spectroscopy), and 4-cyano-4-(thiobenzoylthio)pentanoic acid (CPADB, 97 %) were purchased from Strem Chemicals (Cambridge, UK). Bis(2-(methacryloyloxy)ethyl disulfide monomer (DSDMA) monomer[32] and 4-cyano-4-(thiobenzoyl) sulfanyl) pentanoic succinimide ester (SCPDB)[39] agent were synthesized according to previously reported protocols. 4,4'-Azobis(4-cyanopentanoic acid) ACVA; V-501; 99 %) D_2O and anhydrous ethanol (99 %) were purchased from Sigma-Aldrich (UK). CD_3OD (99.8 %) and CD_2Cl_2 (99.8 %) were purchased from Goss Scientific (Nantwich, UK) and used as received. All solvents were of HPLC quality; they were purchased from Fisher Scientific (Loughborough, UK) and used as received.

Methods

Synthesis of 4-cyano-4-((thiobenzoyl)sulfanyl)pentanoic succinimide ester (SCPDB)

4-Cyano-4-(phenylcarbonothioylthio)pentanoic acid (CPADB, 2.04 g, 7.3 mmol) and N-hydroxysuccinimide (0.84 g, 7.3 mmol) were co-dissolved in anhydrous dichloromethane (15 mL). Dicyclohexylcarbodiimide (DCC) (1.51 g, 7.3 mmol) was added to this solution and the reaction mixture was stirred at 20^{o}C in the dark for 18 h. The insoluble white by-product was removed by filtration, the remaining solution was concentrated using a rotary evaporator, and the resulting liquid was purified by silica column chromatography using a mixed eluent comprising 4:1 v/v n-hexane/ethyl acetate. A red solid was isolated after evaporation of the solvent (yield = 2.50 g, 91%).

Synthesis of bifunctional disulfide-based dithiobenzoate (DSDB) RAFT CTA

First, all glassware was flame-dried to remove all traces of water. SCPDB (1.34 g, 3.56 mmol) was dissolved in anhydrous dichloromethane (20 mL) in a 100 mL two-neck round-bottomed flask fitted with a dropping funnel under a nitrogen atmosphere. A solution of cystamine (0.249 g, 1.62 mmol) in dichloromethane (20 mL) was added dropwise to the SCPDB solution over a period of approximately 1 h. The reaction solution was stirred for 18 h at 21 °C in the dark. The resulting crude purple product was concentrated by evaporating the dichloromethane under vacuum and purified by column chromatography using a gradient eluent ranging from 1:1 ethyl acetate/n-hexane to pure ethyl acetate. A purple solid was obtained after evaporation of the solvent. (Yield = 740 mg, 67 %). ESI-MS: 675 g mol^{-1}. ^{1}H and ^{13}C NMR spectra are shown in the Supporting information (Figure S1)

Synthesis of $PGMA_{55}$ macro-CTA (G_{55})

CPDB RAFT agent (0.864 g, 3.9 mmol) and GMA monomer (25.0 g, 156.1 mmol) were weighed into a 100 mL round-bottomed flask and purged under N_2 for 30 min. ACVA initiator (218.6 mg, 0.78 mmol; CTA/ACVA molar ratio = 5.0) and anhydrous ethanol (49.6 mL; previously purged with N_2 for 30 min) were then added, and the resulting red solution was degassed for a further 10 min. The flask was subsequently sealed and immersed into an oil bath set at 70 °C. After 100 min, the polymerization was quenched by opening to air, immersing in liquid nitrogen for 30 seconds followed by dilution with methanol (100 mL). A final GMA conversion of 82 % was determined by ^{1}H NMR analysis. The methanolic solution was precipitated into a ten-fold excess of dichloromethane. After filtering and washing with dichloromethane, the crude polymer was dissolved in water and the residual dichloromethane was evaporated under vacuum. The resulting aqueous solution was freeze-dried overnight to yield a pink powder. ^{1}H NMR analysis indicated a mean degree of polymerization of 55 for this PGMA macro-CTA.

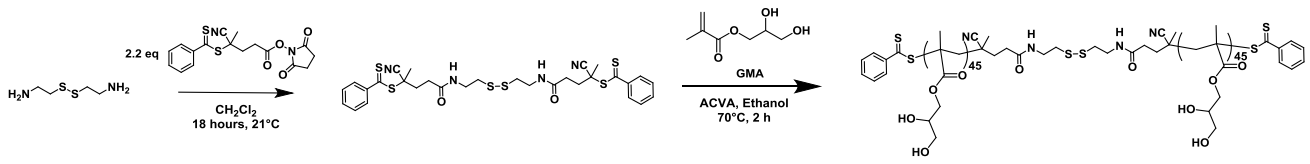

Scheme 2. Synthesis of a disulfide-based bifunctional RAFT agent (DSDB) followed by RAFT solution polymerization of GMA to produce a bifunctional PGMA macro-CTA bearing a central disulfide bond. This is denoted as G_{45}-S-S-G_{45}, or $(G_{45}\text{-S})_2$ for brevity.

Using a refractive index detector and a series of near-monodisperse poly(methyl methacrylate) calibration standards, DMF GPC analysis indicated an M_n of 12,500 g mol^{-1} and an M_w/M_n of 1.23, respectively.

Copolymerization of DSDMA with GMA via RAFT to afford G_{54} -$D_{0.50}$

As an example, a target composition of $PGMA_{54}$-stat-$DS_{0.50}$ was synthesized as follows: CPDB RAFT agent (80 % purity; 0.192 g, 0.69 mmol), GMA monomer (5.00 g, 31.3 mmol) and DSDMA monomer (0.101 g, 0.347 mmol) were weighed into a 100 mL round-bottomed flask and purged under N_2 for 30 min. ACVA initiator (38.9 mg, 0.139 mmol; CTA/ACVA molar ratio = 5.0) and anhydrous ethanol (47.6 mL; previously purged with N_2 for 30 min) were then added and the resulting red solution was degassed for a further 10 min. The flask was subsequently sealed and immersed in an oil bath set at 70 °C. After 18 h, the copolymerization was quenched by immersion in liquid nitrogen. A final GMA conversion of 92 % was determined by ^{1}H NMR analysis. Overnight storage of this ethanolic reaction solution at -25 °C caused precipitation of the $PGMA_{54}$-$DS_{0.50}$, which conveniently allowed decantation of the supernatant solution containing the residual comonomers. This precipitate was dissolved in methanol (100 mL) and then precipitated into a ten-fold excess of dichloromethane. After filtering and washing with dichloromethane, the copolymer was dissolved in water and the residual dichloromethane was evaporated under vacuum. The resulting aqueous solution was freeze-dried to yield a pink powder. ^{1}H NMR (see Figure S2 in the supporting information) analysis of this PGMA macro-CTA indicated a mean degree of polymerization of 54. DMF GPC analysis indicated an M_n of 14,000 g mol^{-1} and an M_w/M_n of 1.26, respectively.

Synthesis of bifunctional PGMA macro-CTA bearing a central disulfide bond $(G_{54}S)_2$

DSDB RAFT agent (0.140 g, 0.208 mmol) and GMA monomer (31.2 mmol, 5.00 g) were weighed into a 50 mL round-bottomed flask and purged under N_2 for 30 min. ACVA initiator (11.7 mg, 0.042 mmol; CTA/ACVA molar ratio = 5.0) and anhydrous ethanol (3.52 mL; previously purged with N_2 for 30 min) were then added, and the resulting red solution was purged for a further 10 min. The flask was subsequently sealed and immersed into an oil bath set at 70 °C. After 100 min, the polymerization was quenched by opening to air, immersing in liquid nitrogen for 30 seconds followed by dilution with methanol (100 mL). A final GMA conversion of 64 % was determined by ^{1}H NMR analysis. The methanolic solution was precipitated into a ten-fold excess of dichloromethane. After filtering and washing with dichloromethane, the crude polymer was dissolved in water and the residual dichloromethane was evaporated under vacuum. The resulting aqueous solution was freeze-dried to yield a pink powder. ^{1}H NMR analysis of the pure solid indicated a mean degree of polymerization of 90 for this macro-CTA (see Figure S2 in the supporting information). DMF GPC analysis indicated an M_n of 20,600 g mol^{-1} and an M_w/M_n of 1.15, respectively.

Synthesis of disulfide-functionalized poly(glycerol monomethacrylate)$_{55}$-poly(2-hydroxypropyl methacrylate)$_{130}$ worm gels via RAFT aqueous dispersion polymerization of HPMA

As an example, [G_{54} -$D_{0.50}$ + (1-x)G_{55}]-H_{130} was synthesized for x = 0.40 as follows: G_{55} macro-CTA (433.6 mg, 0.048 mmol), G_{54} -$D_{0.50}$ macro-CTA (288.6 mg, 0.032 mmol), HPMA monomer (1.50 g, 10.40 mmol; target DP = 130), ACVA (4.50 mg, 0.016 mmol; CTA/ACVA molar ratio = 5.0) and water (20.0 g, to produce a 10.0% w/w aqueous solution) were weighed into a 10 mL round-bottomed flask, which was placed on ice and purged with N_2 for 20 min. Following this degassing protocol, the flask was immersed in an oil bath set at 70 °C. The reaction solution was stirred for 3 h before the RAFT polymerization was quenched by exposure to air.

Reductive cleavage of disulfide bonds within [xG_{54}-$D_{0.50}$ + (1-x)G_{55}]-H_{130}worm gels

For GPC studies: TBP (10 µl, 4 µM) was added to a DMF solution of copolymer (5.0 g dm^{-3}; 2.0 mL) and stirred for 10 minutes under nitrogen prior to GPC analysis. For oscillatory rheology experiments, TCEP was weighed into a sample vial containing the 10 % w/w copolymer gel under a nitrogen atmosphere. The dispersion was placed at 0 °C and stirred for 30 min with a magnetic stirrer bar.

Characterization

NMR All NMR spectra were recorded using a 400 MHz Bruker Avance-400 spectrometer (64 scans averaged per spectrum).

Gel Permeation Chromatography (GPC). Copolymer molecular weights and polydispersities were determined using a DMF GPC set-up operating at 60°C and comprising two Polymer Laboratories PL gel 5 µm Mixed-C columns connected in series to a Varian 390-LC multi-detector suite and a Varian 290-LC pump injection module. The GPC eluent was HPLC grade DMF containing 10 mM LiBr at a flow rate of 1.0 mL min^{-1}. DMSO was used as a flow-rate marker and only the refractive index detector was used. Calibration was conducted using a series of ten near-monodisperse poly(methyl methacrylate) standards (M_n = 625− 618,000 g mol^{-1}). Chromatograms were analyzed using Varian Cirrus GPC software (version 3.3).

Transmission Electron Microscopy (TEM). Copolymer dispersions were diluted fifty-fold at 20°C to generate 0.20% w/w dispersions. Copper/palladium TEM grids (Agar Scientific, UK) were coated in-house to produce a thin film of amorphous carbon. These grids were then treated with a plasma glow discharge for 30 s to create a hydrophilic surface. Each aqueous diblock copolymer dispersion (12 µL; 0.20% w/w) was placed on a freshly-treated grid for 1 min and then blotted with filter paper to remove excess solution. To stain the deposited nano-

particles, an aqueous solution of uranyl formate (9 μL; 0.75% w/w) was placed on the sample-loaded grid via micropipet for 20 s and then carefully blotted to remove excess stain. Each grid was then carefully dried using a vacuum hose. Imaging was performed using a FEI Tecnai Spirit TEM instrument equipped with a Gatan 1kMS600CW CCD camera operating at 120 kV.

Oscillatory Rheology experiments An AR-G2 rheometer equipped with a variable temperature Peltier plate, a 40 ml 2° aluminium cone and a solvent trap was used for all experiments. Loss moduli (G") and storage moduli (G') were measured as a function of applied strain and temperature to identify the linear viscoelastic region and determine the critical gelation temperature (CGT), respectively. Strain sweeps were conducted at constant temperature (5°C) using an angular frequency of 1.0 rad s^{-1}. Angular frequency sweeps were conducted at a constant strain of 1.0 %. Temperature sweeps were conducted at an angular frequency of 1.0 rad s^{-1} and a constant strain of 1.0 %. In the latter experiments, the temperature was increased by 1.0 °C between each measurement, allowing an equilibration time of 2 minutes in each case. The solvent trap was required to prevent evaporation of water over the time scale of the experiment.

Results and Discussion

The G_{54}-$D_{0.50}$ macro-CTA was synthesized at a copolymer concentration of 10 % w/w in order to avoid intermolecular branching.[31] This relatively low concentration retards the rate of copolymerization, but nevertheless ^{1}H NMR spectroscopy studies indicated that >99% comonomer conversion was achieved after 18 h at 70°C in ethanol. Although such high conversions are generally not advisable for RAFT macro-CTA syntheses, in this case it is essential because copolymerization of the second (pendent) methacrylate group on the DSDMA comonomer only occurs at high conversions.[32]

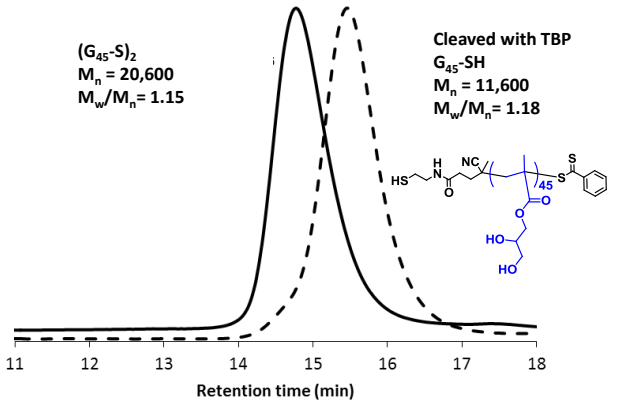

Figure 1. DMF GPC chromatograms obtained for a G_{45}-S-S-G_{45} macro-CTA prior to disulfide cleavage and the G_{45}-SH macro-CTA that is generated on treatment with excess tributylphosphine (TBP).

A number-average molecular weight (M_n) of 14,000 g mol^{-1} and a reasonably low M_w/M_n of 1.26 was recorded for the G_{54}-$D_{0.50}$ macro-CTA, indicating good RAFT control. A small high molecular weight shoulder was observed in the chromatogram, which was ascribed to a low level of branching for this statistical copolymer. A G_{55} macro-CTA was also prepared by RAFT solution polymerization of GMA in ethanol. In this case GPC analysis indicated a comparable molecular weight distribution to that of the G_{54}-$D_{0.50}$ macro-CTA: the M_n was 12,500 g mol^{-1} and the M_w/M_n was 1.23 (see Figure 1).

RAFT aqueous dispersion polymerization of HPMA was conducted using a combination of these two macro-CTAs at various molar ratios, yielding [x$G_{54}$$D_{0.50}$+ (1-x)$G_{55}$]-$H_{130}$ diblock copolymers where the mole fraction of $G_{54}$$D_{0.50}$ (x) ranged from zero to 0.80. In all cases, the resulting aqueous dispersions formed free-standing gels at room temperature and TEM studies of highly dilute dispersions confirmed a pure worm phase in each case (see Figure 2 and Figure S4 in the Supporting Information). Relatively high blocking efficiencies were observed for both macro-CTAs, with the notable absence of any residual macro-CTA signals in the DMF GPC chromatograms (Figure 2). This is a particularly important observation in the case of the G_{54}-$D_{0.50}$ macro-CTA, since the relatively high conversion obtained in this case potentially increases the risk of unwanted termination. If this had occurred, the 'dead' RAFT chain-ends would be expected to produce a low blocking efficiency. Reasonably low copolymer polydispersities were achieved, with a subtle monotonic increase from 1.11 to 1.19 being observed as the proportion of G_{54}-$D_{0.50}$ was increased as a result of low levels of branched copolymer. This is evident from the high molecular weight shoulder, which systematically increases with G_{54}-$D_{0.50}$ mole fraction (see Figure 1).

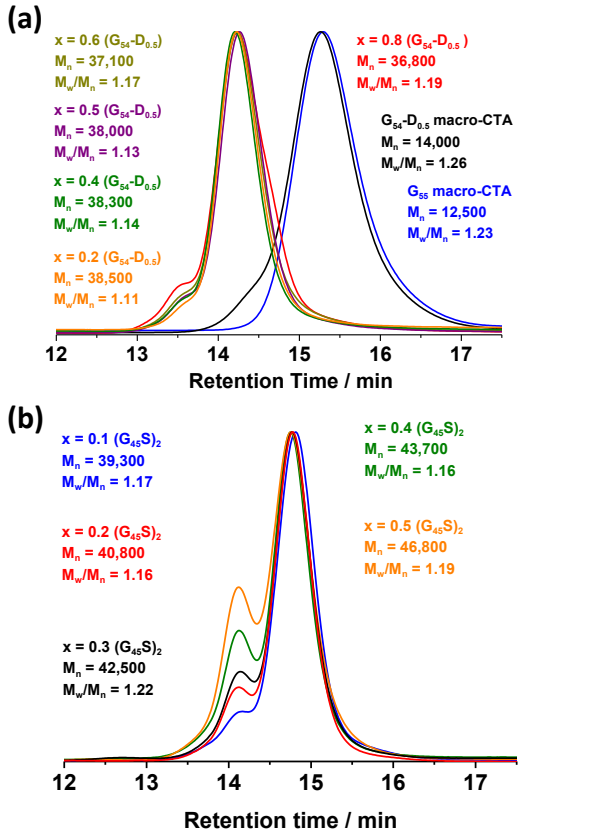

Figure 2. DMF GPC chromatograms obtained for a series of (a) [xG_{54} -$D_{0.50}$+ (1-x)G_{55}]-H_{130} and (b) [x($G_{45}S_2$) + (1-x)G_{55}]-H_{130} diblock copolymers prepared via RAFT aqueous dispersion polymerization of HPMA using various binary mixtures of G_{55} macro-CTA in turn with each of the two disulfide-based macro-CTAs.

The second route to disulfide-functionalized worms involved using a disulfide-based dithiobenzoate (DSDB). This bifunctional CTA was synthesized by coupling the pendent amine groups of cystamine with the activated ester group on a dithiobenzoate-based RAFT CTA (SCDPB, see Scheme 2). This reaction gave an overall yield of 67 % and the resulting product was judged to be of high purity according to both ^{1}H NMR and ES-MS studies. This DSDB was also used to polymerize GMA by ethanolic solution polymerization. The reaction was quenched after 2.5 h, at which point ^{1}H NMR analysis indicated 83% monomer conversion. A $(G_{45}\text{-}S)_2$ macro-CTA was obtained following precipitation into excess dichloromethane, as judged by ^{1}H NMR end-group analysis of the purified polymer.

DMF GPC indicated an M_n of 20,600 g mol^{-1} and a M_w/M_n of 1.15 for this bifunctional macro-CTA. Reductive cleavage of the central disulfide bond in this macro-CTA with excess tributylphosphine produced a reduction in M_n to 11,600 g mol^{-1} with an associated modest increase in M_w/M_n up to 1.18. These observations are consistent with a well-defined bifunctional macro-CTA and further suggest that the DSDB CTA contained negligible levels of monofunctional impurity. Finally, it is noteworthy that the M_n of the thiol-functional polymer chains is comparable to that of the non-functionalized G_{55} macro-CTA (12,500 g mol^{-1}).

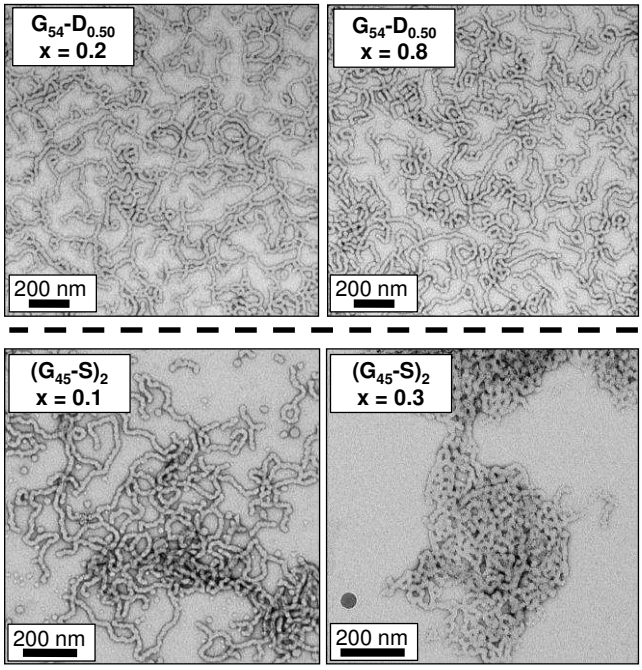

Figure 3. TEM images obtained from selected disulfide functionalized worm gels containing either G_{54}-$D_{0.50}$ or $(G_{45}\text{-}S)_2$ as the disulfide source.

A series of $[x(G_{45}\text{-}S)_2 + (1\text{-}xG_{55})]$–$H_{130}$ diblock copolymer dispersions were prepared using this binary mixture of macro-CTAs, where x was varied between 0.10 and 0.50. Free-standing gels were obtained in all cases apart from the formulation containing 50% $(G_{45}\text{-}S)_2$, which formed a turbid precipitate.

As expected, DMF GPC chromatograms obtained for the various copolymers had bimodal distributions, indicating the presence of both the $(H_{130}\text{-}G_{45}\text{-}S)_2$ triblock and the G_{55}-H_{130} diblock copolymer chains. Normalizing the signal at shorter retention time enables the relative increase in the proportion of $(H_{130}\text{-}G_{45}\text{-}S)_2$ triblock in each case to be clearly visualized. A systematic increase in M_n from 39,300 to 46,800 is observed as x is increased from 0.10 to 0.50, with an associated increase in polydispersity as a result of the increasing proportion of triblock copolymer. Cleavage of the disulfide bonds using excess tributylphosphine allowed comparison of the G_{54}-H_{130} chains with the HS-G_{45}-H_{130} chains (see Figure S3 in the Supporting Information). The presence of a unimodal GPC signal indicates that these two species are comparable in molecular weight. Moreover, there is a significantly smaller increase in M_n with x. This increase is likely to be associated with the presence of low levels of non-cleaved triblock, which increases the final M_n. The polydispersities for these disulfide-cleaved copolymers are always lower because of the removal of the high molecular weight triblock species.

TEM studies confirmed that all dispersions comprised pure worm phases (see Figure 3). When making up these TEM grids, it was significantly easier to prepare samples containing lower levels of the $(G_{45}\text{-}S)_2$ macro-CTA, presumably because these dispersions contained fewer inter-worm disulfide bonds. This appears to be reflected in the TEM images, where the worms tend to form clusters at a $(G_{45}\text{-}S)_2$ mole fraction of 0.30.

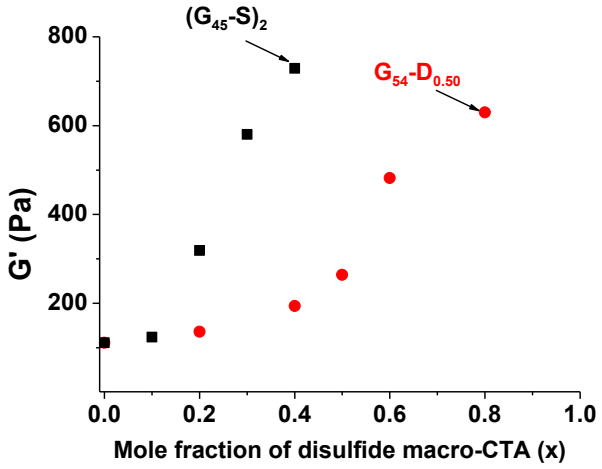

Figure 4. Change in worm gel modulus (G') on varying the fraction of disulfide-functionalized macro-CTA at 25°C. Strain sweeps were conducted at an angular frequency of 1.0 rad s^{-1}.

However, this observation should be treated with some caution, since similar worm clustering has been observed for linear PGMA-PHPMA worm gels that contain no disulfide bonds.[14]

Rheological Properties of Disulfide-based Worm Gels

A pre-requisite for reliable rheological characterization is that measurements are conducted within the linear viscoelastic regime, where the gel moduli (i.e., G' and G") remain independent of strain. Strain sweeps were conducted on all worm gels at a constant angular frequency of 1.0 rad s^{-1}. Each gel exhibited a linear viscoelastic region up to an applied strain of at least 30 % (see Figure S5 in the Supporting Information). From these data, it was possible to examine relative gel strengths by plotting G' against the mole fraction (x) of disulfide bonds (see Figure 4). The $x(G_{54}\text{-}D_{0.5})$ worm gels exhibited a systematic increase in G' from 120 Pa up to 650 Pa as x was varied from 0.20 to 0.80. However, a more pronounced effect

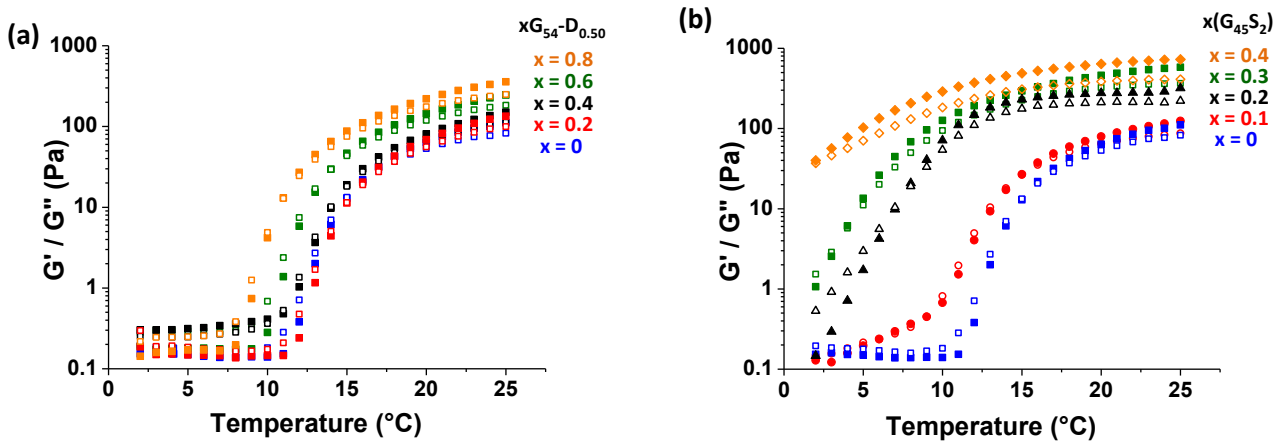

Figure 5. Storage moduli (G', closed symbols) and loss moduli (G", open symbols) obtained via temperature-dependent oscillatory rheology studies on cooling 10 % w/w aqueous dispersions of (a) $[xG_{54}\text{-}D_{0.5}\ (1\text{-}xG_{55})]\text{–}H_{130}$ and (b) $[x(G_{45}\text{-}S)_2\ (1\text{-}xG_{55})]\text{–}H_{130}$ worm gels from 25°C to 2°C. Applied strain = 1.0 % and angular frequency = 1.0 rad s^{-1}.

on gel strength was observed for $(G_{45}\text{-}S)_2$ worm gel series, for which a G' of 740 Pa was recorded at x = 0.40.

Temperature-dependent rheology studies also allow the effect of disulfide cross-linking on the thermo-responsive behavior of the gel to be assessed. For example, in the case of the $x(G_{54}\text{-}D_{0.5})$ worm gel, increasing x from below 0.40 up to 0.80 produces a subtle reduction in the critical gelation temperature from 16°C to 12°C. However, this approach did not generate sufficient inter-worm interactions to prevent complete degelation via a worm-to-sphere transition at lower temperatures.[13] In contrast, incorporation of the $(G_{45}\text{-}S)_2$ macro-CTA had a much more pronounced effect on the CGT, with this thermal transition no longer observed when x = 0.40. Presumably, there are sufficient disulfide linkages between adjacent worms to prevent the worm-to-sphere transition in this case.

To assess the influence of the disulfide bonds on the worm gel strength, selected gels were treated with a ten-fold excess of tris(carboxyethyl)phosphine (TCEP) at pH 7. This reducing reagent selectively cleaves disulfide bonds to produce two thiol groups. In principle, this should remove all inter-worm covalent linkages and hence yield merely physical worm gels of significantly lower gel strength. In both cases, these TCEP experiments caused significant changes in rheological behavior (see Figure 6), with both worm gels becoming much weaker.

In particular, the rheological behavior of a $[0.46G_{45}\text{-SH} + 0.54G_{55}]\text{-}H_{130}$ worm gel (obtained via disulfide cleavage of $[0.30(G_{45}\text{-}S)_2 + 0.70G_{55}]\text{-}H_{130}$ worms) is comparable to that of non-functionalized $G_x\text{-}H_y$ worms containing no disulfide/thiol bonds. Hence these observations provide strong experimental evidence that (i) inter-worm disulfide bonds play a major role in determining the overall worm gel strength and (ii) this contribution can be delineated via appropriate selective bond cleavage experiments.

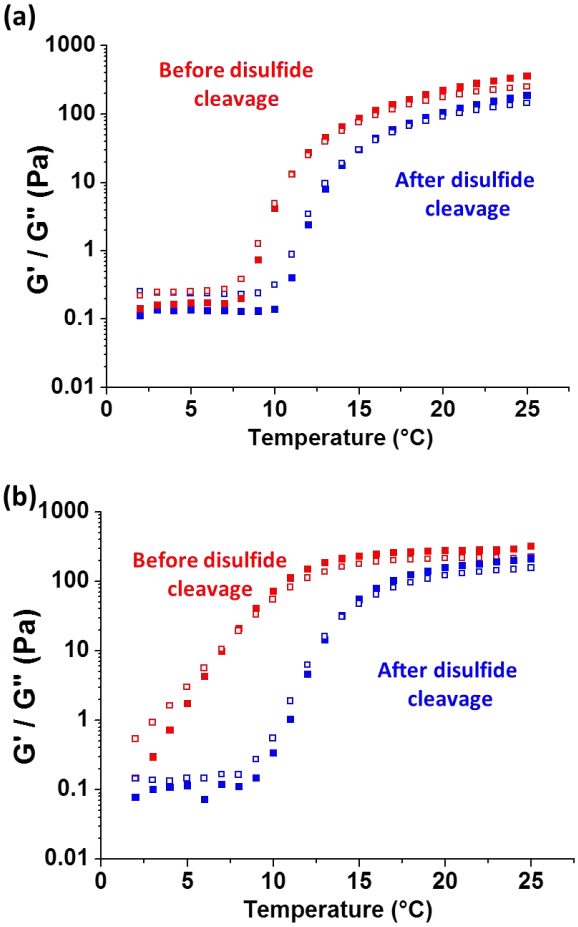

Figure 6. Effect of reductive disulfide cleavage on the rheological properties of (a) $[0.8G_{54}\text{-}D_{0.5}\text{+}0.2G_{55}]\text{-}H_{130}$ and (b) $[0.3(G_{45}\text{-}S)_2]\text{+}0.2G_{55}]\text{-}H_{130}$ worm gels.

Conclusions

Two synthetic protocols were examined to prepare disulfide-functionalized $G_x\text{-}H_y$ diblock copolymer worm gels. Copolymerization of a small amount of bifunctional DSDMA monomer with GMA via RAFT solution polymerization in

ethanol produced a reasonably well-defined G_{54}-$D_{0.50}$ macro-CTA containing approximately 0.50 intramolecular DSDMA cycles per chain. Alternatively, a bifunctional disulfide-based RAFT chain transfer agent was utilized to polymerize GMA in ethanol to produce a bifunctional G_{45} macro-CTA bearing a central disulfide bond.

These two disulfide-based macro-CTAs were used in turn with varying proportions of a non-disulfide-based $PGMA_{55}$ macro-CTA for the RAFT aqueous dispersion polymerization of HPMA. The resulting amphiphilic diblock copolymers self-assembled in situ to form worms, as judged by TEM studies. Soft worm gels could be obtained up to a maximum of 80 mol % G_{54}-$D_{0.50}$ relative to G_{55} macro-CTA. However, only 40 mol % $(G_{45}\text{-}S)_2$ could be incorporated for worm gel syntheses before macroscopic precipitation was observed.

Oscillatory rheology studies confirmed that the incorporation of disulfide bonds into worm gels enabled their gel strength to be significantly enhanced. This is because cleavage of intra-worm disulfide bonds within the stabilizer chains produces thiol groups, which can then recombine to form inter-worm disulfide bonds. Such covalently cross-linked worm gels proved to be up to five-fold stronger than non-functionalized worm gels. Moreover, this increase in gel strength could be readily reversed via reductive disulfide cleavage using excess TCEP at pH 7. This produced thiol-functionalized worm gels of comparable gel strength to that of the non-functionalized worm gels. We envisage that such worm gels should be useful for various biomedical applications, which will be discussed elsewhere in due course.

ASSOCIATED CONTENT

Supporting Information.
^{1}H and ^{13}C NMR spectra recorded for DSDB, ^{1}H spectra for the disulfide-based macro-CTAs, additional TEM, GPC and Rheology data. This material is available free of charge via the Internet at http://pubs.acs.org.

AUTHOR INFORMATION

Corresponding Author

s.p.armes@sheffield.ac.uk

Present Addresses

†If an author's address is different than the one given in the affiliation line, this information may be included here.

Funding Sources

EPSRC is thanked for post-doctoral support of NJW (EP/L024160/1). SPA acknowledges a five-year ERC Advanced Investigator grant (PISA 320372).

REFERENCES

(1) Charleux, B.; Delaittre, G.; Rieger, J.; D'Agosto, F. Macromolecules **2012**, 45, 6753.

(2) Blanazs, A.; Madsen, J.; Battaglia, G.; Ryan, A. J.; Armes, S. P. Journal of the American Chemical Society **2011**, 133, 16581.

(3) Blanazs, A.; Ryan, A. J.; Armes, S. P. Macromolecules **2012**, 45, 5099.

(4) Li, Y.; Armes, S. P. Angewandte Chemie International Edition **2010**, 49, 4042.

(5) Sugihara, S.; Blanazs, A.; Armes, S. P.; Ryan, A. J.; Lewis, A. L. Journal of the American Chemical Society **2011**, 133, 15707.

(6) Figg, C. A.; Simula, A.; Gebre, K. A.; Tucker, B. S.; Haddleton, D. M.; Sumerlin, B. S. Chemical Science **2015**, 6, 1230.

(7) Pei, Y.; Sugita, O. R.; Thurairajah, L.; Lowe, A. B. RSC Advances **2015**, 5, 17636.

(8) Shen, W.; Chang, Y.; Liu, G.; Wang, H.; Cao, A.; An, Z. Macromolecules **2011**, 44, 2524.

(9) Wan, W.-M.; Pan, C.-Y. Polymer Chemistry **2010**, 1, 1475.

(10) Kang, Y.; Pitto-Barry, A.; Willcock, H.; Quan, W. D.; Kirby, N.; Sanchez, A. M.; O'Reilly, R. K. Polymer Chemistry **2015**, 6, 106.

(11) Warren, N. J.; Mykhaylyk, O. O.; Mahmood, D.; Ryan, A. J.; Armes, S. P. Journal of the American Chemical Society **2013**.

(12) Ladmiral, V.; Charlot, A.; Semsarilar, M.; Armes, S. P. Polymer Chemistry **2015**, 6, 1805.

(13) Blanazs, A.; Verber, R.; Mykhaylyk, O. O.; Ryan, A. J.; Heath, J. Z.; Douglas, C. W. I.; Armes, S. P. Journal of the American Chemical Society **2012**, 134, 9741.

(14) Verber, R.; Blanazs, A.; Armes, S. P. Soft Matter **2012**, 8, 9915.

(15) Jia, Z.; Bobrin, V. A.; Truong, N. P.; Gillard, M.; Monteiro, M. J. Journal of the American Chemical Society **2014**, 136, 5824.

(16) Chen, X.; Prowse, A. B. J.; Jia, Z.; Tellier, H.; Munro, T. P.; Gray, P. P.; Monteiro, M. J. Biomacromolecules **2014**, 15, 844.

(17) Zou, J.; Hew, C. C.; Themistou, E.; Li, Y.; Chen, C.-K.; Alexandridis, P.; Cheng, C. Advanced Materials **2011**, 23, 4274.

(18) Lowe, A. B. Polymer Chemistry **2010**, 1, 17.

(19) Kade, M. J.; Burke, D. J.; Hawker, C. J. Journal of Polymer Science Part A: Polymer Chemistry **2010**, 48, 743.

(20) Hoyle, C. E.; Bowman, C. N. Angewandte Chemie International Edition **2010**, 49, 1540.

(21) Sumerlin, B. S.; Vogt, A. P. Macromolecules **2009**, 43, 1.

(22) Iha, R. K.; Wooley, K. L.; Nyström, A. M.; Burke, D. J.; Kade, M. J.; Hawker, C. J. Chemical Reviews **2009**, 109, 5620.

(23) Killops, K. L.; Campos, L. M.; Hawker, C. J. Journal of the American Chemical Society **2008**, 130, 5062.

(24) Kolb, H. C.; Sharpless, K. B. Drug Discovery Today **2003**, 8, 1128.

(25) Li, M.; De, P.; Li, H.; Sumerlin, B. S. Polymer Chemistry **2010**, 1, 854.

(26) Willcock, H.; O'Reilly, R. K. Polymer Chemistry **2010**, 1, 149.

(27) Warren, N. J.; Armes, S. P. Journal of the American Chemical Society **2014**, 136, 10174.

(28) Grover, G. N.; Lee, J.; Matsumoto, N. M.; Maynard, H. D. Macromolecules **2012**, 45, 4958.

(29) Rosselgong, J.; Blanazs, A.; Chambon, P.; Williams, M.; Semsarilar, M.; Madsen, J.; Battaglia, G.; Armes, S. P. ACS Macro Letters **2012**, 1, 1041.

(30) Matsumoto, N. M.; Gonzalez-Toro, D. C.; Chacko, R. T.; Maynard, H. D.; Thayumanavan, S. Polymer Chemistry **2013**, 4, 2464.

(31) Rosselgong, J.; Armes, S. P.; Barton, W. R. S.; Price, D. Macromolecules **2010**, 43, 2145.

(32) Rosselgong, J.; Armes, S. P.; Barton, W.; Price, D. Macromolecules **2009**, 42, 5919.
(33) Rosselgong, J.; Armes, S. P. Macromolecules **2012**, 45, 2731.
(34) Li, C.; Buurma, N. J.; Haq, I.; Turner, C.; Armes, S. P.; Castelletto, V.; Hamley, I. W.; Lewis, A. L. Langmuir **2005**, 21, 11026.
(35) Madsen, J.; Armes, S. P.; Bertal, K.; Lomas, H.; MacNeil, S.; Lewis, A. L. Biomacromolecules **2008**, 9, 2265.
(36) Madsen, J.; Armes, S. P.; Lewis, A. L. Macromolecules **2006**, 39, 7455.
(37) Irmukhametova, G. S.; Mun, G. A.; Khutoryanskiy, V. V. Langmuir **2011**, 27, 9551.
(38) Storha, A.; Mun, E. A.; Khutoryanskiy, V. V. RSC Advances **2013**, 3, 12275.
(39) Warren, N. J.; Mykhaylyk, O. O.; Mahmood, D.; Ryan, A. J.; Armes, S. P. Journal of the American Chemical Society **2013**, 136, 1023.

.

Insert Table of Contents artwork here